JACS
JOURNAL OF THE AMERICAN CHEMICAL SOCIETY

Article

pubs.acs.org/JACS

Cooperativity and Complexity in the Binding of Anions and Cations to a Tetratopic Ion-Pair Host

Ethan N. W. Howe,[†] Mohan Bhadbhade,[‡] and Pall Thordarson*,[†]

[†]School of Chemistry, The University of New South Wales, Sydney, NSW 2052, Australia

[‡]Mark Wainwright Analytical Centre, The University of New South Wales, Sydney, NSW 2052, Australia

Supporting Information

ABSTRACT: Cooperative interactions play a very important role in both natural and synthetic supramolecular systems. We report here on the cooperative binding properties of a tetratopic ion-pair host **1**. This host combines two isophthalamide anion recognition sites with two unusual "half-crown/two carbonyl" cation recognition sites as revealed by the combination of single-crystal X-ray analysis of the free host and the 1:2 host:calcium cation complex, together with two-dimensional NMR and computational studies. By systematically comparing all of the binding data to several possible binding models and focusing on four different variants of the 1:2 binding model, it was in most cases possible to quantify these complex cooperative interactions. The data showed strong negative cooperativity (α = 0.01−0.05) of **1** toward chloride and acetate anions, while for cations the results were more variable. Interestingly, in the competitive ($CDCl_3/CD_3OD$ (9:1, v/v)) solvent, the addition of calcium cations to the tetratopic ion-pair host **1** allosterically switched "on" chloride binding that is otherwise not present in this solvent system. The insight into the complexity of cooperative interactions revealed in this study of the tetratopic ion-pair host **1** can be used to design better cooperative supramolecular systems for information transfer and catalysis.

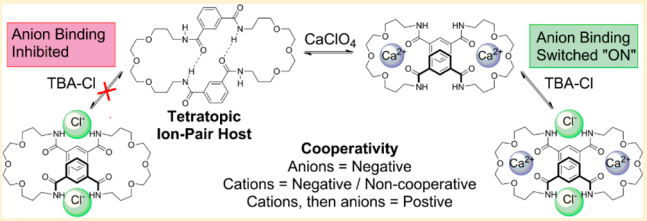

INTRODUCTION

Cooperative interactions play a very significant role in many natural processes[1] where information transfer between biological complexes takes place. From the sigmoidal binding response of the hemoglobin tetramer to oxygen pressure,[2] to the allosteric binding of cyclic AMP to the gene transcription-regulating cAMP receptor protein (CRP) to DNA,[3] researchers continue to unravel a dazzling array of how the binding of a small molecule to one particular site in a complex can influence its function at another remote site as the binding information is transmitted. The study of cooperative interactions has also played a major role within the field of supramolecular chemistry[4] and even in the case of relatively simple small-molecule host−guest interactions; fundamental questions regarding cooperative binding continue to challenge and fascinate researchers.[1a,5]

The archetypical host−guest system for the investigation of cooperative binding is the formation of a 1:2 host (receptor)−guest (ligand) complex HG_2.[5b,6] The binding of two guests to a host can then be subdivided further depending on whether the two guests are identical (homotropic) or not (heterotropic). In principle, all that is required is to compare, after correcting for statistical factors, are the stepwise association constants (e.g., K_1 and K_2) for the formation of the 1:1 (HG) and 1:2 (HG_2) complex and to see if these differ.[5b,6] If the first binding event does appear to influence the second, one can move on to explaining the origin of the observed cooperativity, be they the results of guest−guest interactions, structural allosteric changes in the host, or other factors. In practice, however, even the determination of these stepwise binding constants is not always straightforward; one often overlooked issue is if the fitting data for 1:2 binding allow for the inclusion of the additional fitting parameters that are required to extract stepwise binding constants.[6d]

Ion-pair hosts (receptors)[7] are molecules that have recognition sites for both cations and anions and hence provide another fascinating platform for the study of cooperativity. Electrostatic repulsion is a common problem in the binding of two or more ions of the same kind (e.g. two anions) to a host, resulting in negative homotropic cooperativity regardless of the nature of the host. In ion-pair hosts, however, positive heterotropic cooperativity is often observed instead,[7b,8] as attractive forces between the cation and anion species dominate the overall equilibria. The vast majority of ion-pair hosts reported to date are ditopic,[7b,8,9] binding one cation and one anion, supplemented with a few examples of tritopic ion-pair hosts.[7a,10] Tetratopic ion-pair hosts have remained elusive, despite the obvious appeal they have in terms of investigating cooperativity in complex settings.

To address some of the questions raised above concerning cooperative binding, we report here a new synthetic tetratopic ion-pair macrocyclic host **1**. The design of **1** was based on the tritopic host reported by Lüning and co-workers,[10b] with a

Received: April 4, 2014
Published: May 5, 2014

crown-6 instead of a crown-4 used in **1** to combine two isophthalamide anion binding sites. Using crown-6 allowed us to study the binding of two cations and two anions simultaneously to the tetratopic ion-receptor **1**. This design allowed us then to study the cooperativity of cation binding, anion binding, and the combination of both in a single, well-defined host system.

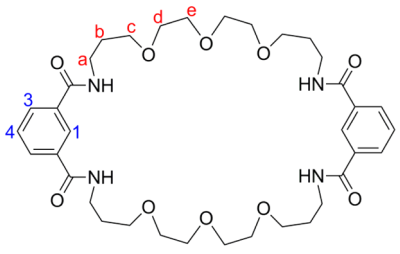

1

In all cases, we have also performed a detailed analysis of the validity of the different binding models[6d] that can be used to describe the possible 1:1 and 1:2 equilibria present (Table 1) and whether they point to cooperativity. We hope to show that this approach will be of use in studying 1:2 binding phenomena. We also demonstrate how the nature of the solvent influences anion and cation binding cooperativity in host **1**, which in most cases is negative. We then show that positive heterotopic cooperativity between cations and anions can switch "on" anion binding in a competitive solvent and switch cooperativity between two anions from negative to positive cooperativity as evident by the sigmoidal binding isotherms observed.

RESULTS AND DISCUSSION

Binding Models Discussed in This Work and Their Selection. Before proceeding further, a short description will be given of the different binding models outlined in Table 1 (see also Supporting Information Table S2) and used in this study. In most cases, five binding models were considered: the simple 1:1 binding model and four different variants of the 1:2 binding model. The difference between these four variants is in terms of whether the two stepwise binding constants (K_1 and K_2) are linked ($K_1 = 4K_2$) and whether the stepwise changes in ^{1}H NMR resonances (the induced chemical shifts $\delta_{\Delta HG}$ and $\delta_{\Delta HG_2}$ for the formation of a 1:1 and 1:2 complex, respectively) are linked ($2\delta_{\Delta HG} = \delta_{\Delta HG_2}$). Whether these parameters are linked determines in turn how many parameters are obtained from the nonlinear regression fitting process. This is important because if the different models are only compared in terms of the quality of fit, the binding model variant with the largest number of fitted parameters would usually appear to fit the data best. Hence, both the overall quality of fit and the number of fitted parameters ($n-df$, where n = number of data points fitted and df = degrees of freedom) need to be considered when determining which binding model(s) fit the data best.

All of the binding data presented here have been fitted using *fittingprogram*,[6c] which is a custom written Matlab-based global analysis nonlinear regression program that solves explicitly the relevant equations for 1:2 equilibria. The global analysis approach means that binding isotherms corresponding to several proton resonances of interest are minimized simultaneously, ensuring a much more robust fitting process than if only one binding isotherm is used for fitting (local analysis).[6c,d,11] This does, however, impact on the number of fitted parameters ($n-df$), and hence the comparison between the different binding models analyzed here as shown in Table 1.

For each data set, the quality of fit versus the number of fitted parameters ($n-df$) is then compared to arrive at one or two (and rarely three) plausible binding models for that particular data set, which then form the basis of the discussion below (see also the Supporting Information for further details on these binding models and the process used to identify the most plausible binding models).

Synthesis and Solid-State Structural Analysis. The macrocyclic host **1** was synthesized in 7% yield via a concerted tetra-amide formation from 2 equiv of the isophthaloyl dichloride **2** and 2 equiv of tri(ethylene glycol) diamine **3** under high dilution conditions (see Supporting Information Scheme S1). The smaller crown-3-isophtahalimide macrocycle **4** (previously reported)[12] was also isolated in 32% yield from this reaction. The high resolution electrospray ionization mass spectrometry (HR–ESI–MS) analysis has shown evidence of cation and anion binding capabilities from the formation of $[\mathbf{1} + Na]^+$ (m/z = 723.3516) and $[\mathbf{1} + Cl]^-$ (m/z = 735.3328) adducts with the highest abundance in the positive and negative modes, respectively (see Supporting Information Figure S1).

Table 1. Different Binding Model Compared in this Work

	relationship between		number of fitted parameters ($n-df$) and number of isotherms used in the global fitting process			
binding model	K_1 and K_2	$\delta_{\Delta HG}$ and $\delta_{\Delta HG_2}$ [a]	one	two	three	four
1:1	N/A[b]	N/A[b]	2	3	4	5
statistical 1:2	$K_1 = 4K_2$	$\delta_{\Delta HG_2} = 2\delta_{\Delta HG}$	2	3	4	5
noncooperative 1:2	$K_1 = 4K_2$	$\delta_{\Delta HG_2} \neq 2\delta_{\Delta HG}$	3	5	7	9
additive 1:2	$K_1 \neq 4K_2$	$\delta_{\Delta HG_2} = 2\delta_{\Delta HG}$	3	4	5	6
full 1:2	$K_1 \neq 4K_2$	$\delta_{\Delta HG_2} \neq 2\delta_{\Delta HG}$	4	6	8	10
full 2:1[c]	$K_1 \neq 4K_2$	$\delta_{\Delta HG_2} \neq 2\delta_{\Delta HG}$	4	6	8	10

[a]The $\delta_{\Delta HG}$ and $\delta_{\Delta HG_2}$ denote the changes in the NMR resonance(s) of interest upon forming a 1:1 ($\delta_{\Delta HG}$) and 1:2 ($\delta_{\Delta HG_2}$) complex. [b]For the 1:1 binding model, there is only one binding constant (K_1) and one change in NMR resonance(s), $\delta_{\Delta HG}$. In this work, the 1:1 binding model is used as a benchmark to which all of the other models are compared. [c]The full 2:1 binding model mirrors the full 1:2 model, except that a formation of a 2:1 host–guest (H_2G) instead of a 1:2 host–guest (HG_2) is assumed as the final product. This particular binding model was only considered in the case of sodium (Na^+) cation binding to **1** in the $CDCl_3/CD_3OD$ (9:1, v/v) solvent system (see below). See also the Supporting Information for more details.

dx.doi.org/10.1021/ja503383e | J. Am. Chem. Soc. 2014, 136, 7505–7516

Colorless thin plates of host **1** suitable for single-crystal X-ray structure determination were grown from slow diffusion of diethyl ether into a solution of **1** in dichloromethane. The structure of **1** as a free host crystallizes in the orthorhombic space group *Pccn* with the resolved molecular structure as shown in Figure 1a. The solid-state structure shows that the

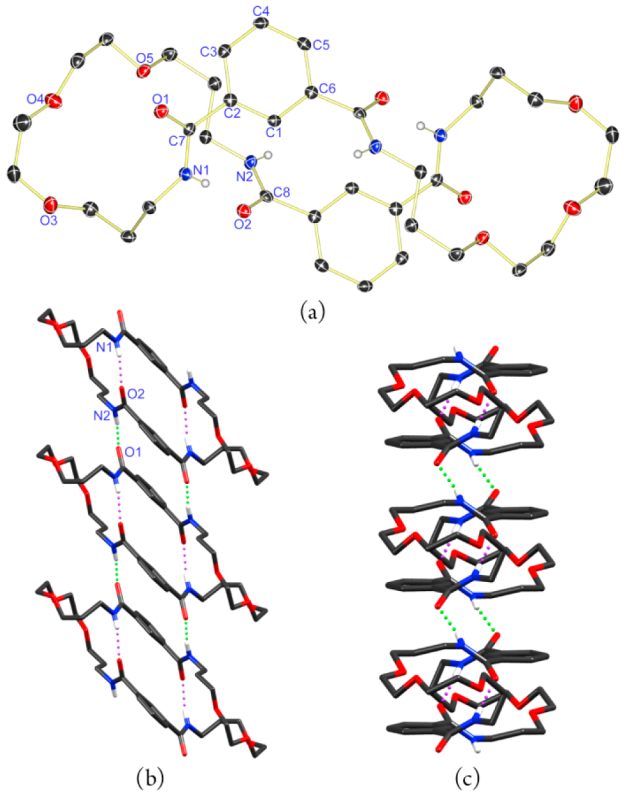

Figure 1. Molecular structure of host **1** derived from the single-crystal X-ray analysis: (a) ORTEP diagram showing 50% probability anisotropic displacement ellipsoids at 100(2) K and (b,c) perspective packing diagrams showing the intramolecular and intermolecular hydrogen-bond interactions. All H atoms are omitted for clarity, except amide-H showing intramolecular (purple dots) and intermolecular (green dots) hydrogen bonds. Selected hydrogen bond distances (Å), bond angles (deg), and torsion angles (deg): N(1)H···O(2) 2.087(1), N(2)H···O(1) 2.026(1); C(7)−N(1)−H 118.3(1), C(8)−N(2)−H 118.1(1); C(3)−C(2)−C(7)−O(1) 32.3(2), C(5)−C(6)−C(8)−O(2) 37.8(2). Symmetry transformation used to generate equivalent atoms: A, $-x + 1$, $-y + 1$, $-z + 1$.

centrosymmetric macrocycle has an interesting folded-closed conformation locked by two intramolecular hydrogen bonds between the four carboxamides linking the two isophthalamide moieties in proximity. The intramolecular NH···O hydrogen-bond lengths (2.087 Å) are slightly longer in contrast to the intermolecular NH···O hydrogen-bond distances (2.026 Å). The two aromatic rings are oriented in a parallel highly offset arrangement, with a large aromatic centroid distance (6.233 Å) suggesting weak or no $\pi-\pi$ interactions. The unit cell packing (see Supporting Information, Figure S4) further shows neither the presence of ion guest inclusion nor cocrystallizing solvents.

Anion Binding and Solvent Effect. Using ^{1}H NMR spectroscopy, the binding of various anions with host **1** in solution was initially studied in DMSO-d_6/acetone-d_6 (1:9, v/v), a noncompetitive aprotic solvent environment for anion binding. Preliminary titrations of **1** (1.0 mM) with tetrabutylammonium (TBA) anion salts caused the resonances of the amide-H and aromatic-H1 to shift downfield, indicative of anion binding within the cleft of the isophthalamide binding site via hydrogen-bond interactions with the carboxamides.[13] At 2 equiv of TBA-anion salts, the induced shifts from the addition of TBA-chloride (TBA-Cl) and TBA-acetate (TBA-OAc) are more prominent than TBA-bromide (TBA-Br), iodine (TBA-I), and nitrate (TBA-NO_3) (see Supporting Information, Figure S26). Furthermore, TBA-OAc resulted in a larger change in the resonance of amide-H when compared to TBA-Cl, while the shift of aromatic-H1 is smaller. This suggests the smaller chloride binds closer within the cleft, while the larger acetate anion forms stronger hydrogen-bond interactions with the amide-H.

Titration studies with TBA-ClO_4 and TBA-PF_6 were performed as control experiments to demonstrate that these noncoordinating anions did not induce any resonance shifts even with a significantly high excess of 50 equiv. It is noteworthy to mention that the ethyleneoxy proton ($-OCH_2CH_2-$) resonances did not have any significant shift upon the addition of the TBA-salts (see Supporting Information Figure S27), indicating no complexation of TBA cation within the crown ether cavity of host **1**, and that binding of anions did not result in any drastic conformational perturbation of the macrocycle in solution.

With two isophthalamide moieties, host **1** provides two potential anion binding sites. Three repeats of ^{1}H NMR titrations of **1** with the strongly interacting TBA-OAc and TBA-Cl salts in four different solvent systems were performed, focusing on the shifts in the resonances of amide-H and aromatic-H1. The data were then fitted to both the 1:1 model and the four variants of the 1:2 models shown in Table 1 (see the Supporting Information for a detailed description). Comparing the fits and the number of parameters (see Supporting Information Tables S3−S11 and Figures S6−S14) indicated as shown in Table 2 that only the full 1:2 and additive 1:2 models needed to be considered for anion binding to **1** in the DMSO-d_6/acetone-d_6 (1:9, v/v), $CDCl_3$/CD_3CN (1:9, v/v), and $CDCl_3$/CD_3CN (1:1, v/v) solvent systems. In the most protic solvent mixture investigated, CD_3OD/$CDCl_3$ (1:9, v/v), all of the observed ^{1}H chemical shifts ($\Delta\delta = \delta$(for free **1**) − δ(after adding guest to **1**)) were insignificant ($\Delta\delta < 0.05$ ppm) upon the addition of any TBA-anion salt tested, suggesting no or extremely weak anion binding (K_1 and $K_2 < 1$ M^{-1}) to **1**, even with large excess of the target anions present. The only exception to this was TBA-Cl where a shift of about 0.07 ppm was observed after the addition of more than 100 equiv. Attempts to fit this data were not successful, suggesting that even for TBA-Cl the association constants are likely to be very small. Additionally, the bindings of TBA-Br, TBA-I, and TBA-NO_3^- to **1** in DMSO-d_6/acetone-d_6 (1:9, v/v) were also investigated.

Examination of the results in Table 2 reveals a number of important trends. First, it is noteworthy that for all of the TBA-anion salts, the data clearly fit best to a 1:2 binding model whereby cooperativity is assumed (the full and additive models). From the data obtained, the interaction parameter α is in all cases less than 1, indicative of negative cooperativity.[6a−c] This would most likely be due to electrostatic repulsion between the two anions, inhibiting the second binding event. Additional evidence for this comes from observing the trends in which α values for TBA-OAc and TBA-Cl increase (less negative cooperativity) on going from

dx.doi.org/10.1021/ja503383e | J. Am. Chem. Soc. 2014, 136, 7505−7516

Table 2. Most Plausible Binding Models, Stepwise K_1 and K_2 Association Constants, and Interaction Parameters (α) for the Complexation of Host 1 toward Various Anions (as TBA Salts) Obtained from ^{1}H NMR Titrations (400 MHz) at 298 K in the Solvent Mixtures Shown[a]

salt used	solvent	binding model[b]	K_1 (M^{-1})	K_2 (M^{-1})	α[c]
TBA-OAc	DMSO-d_6/acetone-d_6 (1:9, v/v)	full 1:2	9700 (1200)	18 (16)	0.007
	DMSO-d_6/acetone-d_6 (1:9, v/v)	additive 1:2	10 000 (1800)	27.4 (2.5)	0.01
	$CDCl_3$/CD_3CN (1:9, v/v)	additive 1:2	580 (9)	4.3 (0.2)	0.03
	$CDCl_3$/CD_3CN (1:1, v/v)	additive 1:2	400 (8)	51.5 (3.4)	0.52
	$CDCl_3$/CD_3CN (1:1, v/v)	full 1:2	250 (11)	20.7 (0.5)	0.33
TBA-Cl	DMSO-d_6/acetone-d_6 (1:9, v/v)	full 1:2	5100 (790)	40.6 (9.1)	0.03
	DMSO-d_6/acetone-d_6 (1:9, v/v)	additive 1:2	4500 (530)	20.2 (1.4)	0.02
	$CDCl_3$/CD_3CN (1:9, v/v)	additive 1:2	230 (20)	3.1 (0.6)	0.05
	$CDCl_3$/CD_3CN (1:1, v/v)	additive 1:2	140 (4)	18.2 (1.3)	0.52
	$CDCl_3$/CD_3CN (1:1, v/v)	full 1:2	170 (11)	23.2 (1.6)	0.55
TBA-Br	DMSO-d_6/acetone-d_6 (1:9, v/v)	additive 1:2	640 (29)	35.4 (2.2)	0.22
	DMSO-d_6/acetone-d_6 (1:9, v/v)	full 1:2	830 (150)	47.6 (8.1)	0.23
TBA-I	DMSO-d_6/acetone-d_6 (1:9, v/v)	full 1:2	180 (52)	10.9 (0.4)	0.24
TBA-NO_3	DMSO-d_6/acetone-d_6 (1:9, v/v)	full 1:2	100 (40)	9.6 (3.6)	0.38

[a]The data here are a summary of a more detailed analysis of binding data shown in Supporting Information Tables S3−S11 and Figures S6−S14, and only data for the binding model(s) that fitted best with the experimental data are shown here (see above and Supporting Information for more details). The numbers shown are the rounded averages from triplicate measurements with the standard deviation shown in brackets. [b]See Table 1 and the Supporting Information on details on the difference between these binding models and how the best model(s) are selected. [c]The interaction parameter $\alpha = 4K_2/K_1$ with $\alpha > 1$ indicating positive cooperativity, $\alpha < 1$ negative cooperativity, and $\alpha = 1$ no cooperativity.[6a−c]

the relatively poor electron-accepting DMSO-d_6/acetone-d_6 (1:9, v/v) to the more competitive charge-shielding CD_3OD/$CDCl_3$ (1:9, v/v) solvent system. Irrespective of the exact binding model used, comparison of the association constant K_1 in DMSO-d_6/acetone-d_6 (1:9, v/v) reveals the anion binding strength of **1** decreases in the order of acetate > chloride > bromide > iodide ≈ nitrate; this order is consistent with data for other isophthalamide hosts[13,14] and closely resembles the Hofmeister series, often used to discuss ion specificity in proteins and biology.[15]

Comparison of the binding isotherms for the binding of TBA-OAc and TBA-Cl to **1** in the four different solvent mixtures used showed a decrease in $\Delta\delta$ for the aromatic-H1 with the enhancement of hydrogen-donating nature of the solvent mixture used (see Supporting Information Figures S6,S7 and Figures S11−S14). In the most protic solvent mixture of CD_3OD/$CDCl_3$ (1:9, v/v), $\Delta\delta$ was very small (<0.05 ppm), suggesting extremely weak binding (K_1 and K_2 < 1 M^{-1}) or no association at all.

Using the additive 1:2 data from Table 2 as an example, it is also clear that the binding affinity of both TBA-OAc and TBA-Cl toward **1** was drastically affected when changing from an aprotic solvent mixture of DMSO-d_6/acetone-d_6 (1:9, v/v) to $CDCl_3$/CD_3CN (1:9, v/v), with a 17-fold decrease in K_1 for CH_3COO^- and 20-fold decrease for Cl^- observed. Similarly, increasing the ratio of protic $CDCl_3$ in CD_3CN to 1:1 (v/v) continues to decrease the K_1 for the anions, and eventually quenching (switching "off") the anion binding ability of **1** when the more protic CD_3OD was introduced as earlier mentioned. The calculated binding free energy plot (Figure 2) for both the TBA-OAc and TBA-Cl interestingly displays similar slope trends when plotted against the averaged "acceptor number"[16] of the solvent mixtures, further highlighting the sensitivity and importance of solvent competition and control in the thermodynamic equilibrium binding of host **1** toward anions.

Cation Binding and Conformation Perturbation. When host **1** was initially designed, it was not entirely clear if the crown-6 unit would be capable of binding one or two cations

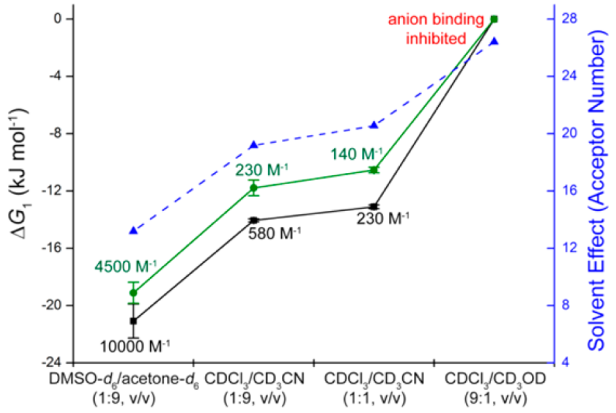

Figure 2. Plot of calculated binding free energy ΔG_1 based on the additive 1:2 model data from Table 2 for the complexation of host **1** toward TBA-OAc (■) and TBA-Cl (green ●) in four solvent mixtures with error bars indicating the expanded uncertainty at the 95% confidence interval. Also shown are the calculated average acceptor numbers[16] (blue ▲) for the solvent mixtures.

such as sodium or calcium. Crown-6-based hosts are known to form 1:2 complexes with various cations,[17] and to ascertain whether **1** could bind to more than one cation, experiments to grow crystals of **1** in the presence of various cation-salts were undertaken with successful results obtained in the presence of calcium perchlorate ($Ca(ClO_4)_2$).

Slow evaporation from a solution of host **1** with excess $Ca(ClO_4)_2$ (10 equiv) in methanol/dichloromethane (1:1, v/v) gave colorless thin plates suitable for single-crystal X-ray diffraction. The resolved X-ray structure (Figure 3a) reveals a 1:2 H:G complex of **1**·2[$Ca(ClO_4)_2$] with the presence of four water molecules, and this centrosymmetric structure crystallizes in the triclinic space group $P\bar{1}$. The inclusion of each Ca^{2+} was established via three oxygen atoms from one tri(ethylene oxide) linkage and two amide-carbonyl oxygen atoms from each individual isophthalamide moiety, along with two axial water ligands giving the seven-coordinate complex. The host **1**

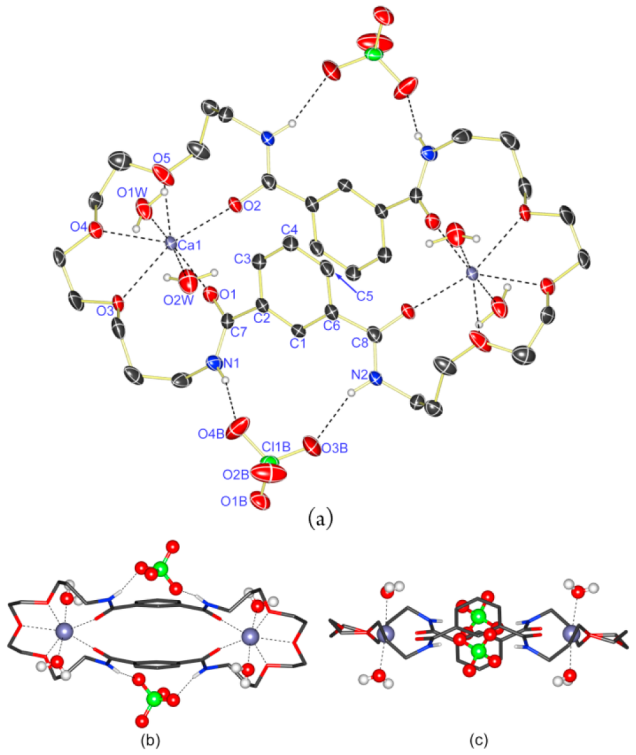

Figure 3. Molecular structure of **1**·2[$Ca(ClO_4)_2$]·4H_2O H:G complex derived from the single-crystal X-ray analysis; two molecules of disordered unbound ClO_4^- anions and all H atoms are omitted for clarity, except amide-H and H_2O. (a) ORTEP diagram showing 50% probability anisotropic displacement ellipsoids at 100(2) K, (b) viewed in the plane of aromatic rings, and (c) viewed in the plane of Ca^{2+} cations. Selected supramolecular contact distances (Å), bond angles (deg), and torsion angles (deg): N(1)H···O(4B) 2.069(5), N(2)H···O(3B) 2.086(4), O(1)···Ca(1) 2.289(4), O(2)···Ca(1) 2.273(4), O(3)···Ca(1) 2.477(4), O(4)···Ca(1) 2.462(3), O(5)···Ca(1) 2.457(4), O(1W)···Ca(1) 2.335(5), O(2W)···Ca(1) 2.351(6), Ca^{2+}···Ca^{2+} 10.337(4); C(7)−N(1)−H 119.7(5), C(8)−N(2)−H 119.3(5); C(3)−C(2)−C(7)−O(1) 30.7(8), C(5)−C(6)−C(8)−O(2) 25.5(8). Symmetry transformation used to generate equivalent atoms: A, $-x + 1$, $-y$, $-z + 1$.

therefore possesses two unusual "half-crown/two carbonyl" cation binding sites with a Ca^{2+}···Ca^{2+} distance of 10.337 Å (Figure 3b). It appears that each Ca^{2+} coordinating site resembles a crown-5-ether complex, often observed with the presence of additional water ligands.[18] The ion-dipole bond lengths between Ca^{2+} and the amide-carbonyl Ca^{2+}···O=C (2.273 and 2.289 Å) are significantly shorter than the Ca^{2+}···O distances (2.457−2.477 Å) from the ethyleneoxy groups, and also shorter in contrast to the aqua ligands (with Ca^{2+}···O distances of 2.335 and 2.351 Å). The torsion angles of the carbonyl bond to the aromatic plane of the bimetallic complex (25.5° and 30.7°) are also much smaller than for the free host **1** (32.3° and 37.8°); see Figures 1 and 3. The two aromatic rings are now oriented in a parallel cofacial offset arrangement with a proximal aromatic centroid distance of 3.569 Å, demonstrating a prevalent $\pi-\pi$ interaction.

Additionally, there are two ClO_4^- anions bound at each of the isophthalamide anion binding sites via hydrogen-bonding interactions (with NH···O distances of 2.069 and 2.086 Å). The binding of these anions to **1** has induced the isophthalamide to adopt the syn−syn configuration,[4e,13b] and also resulted in a larger C−N−H amide bond angle (119.3° and 119.7°) than for the free host (118.1° and 118.3°). The remaining two unbound ClO_4^- anions cocrystallize as "ion-bridges" peripheral to the bimetallic complexes as shown in the unit cell crystallographic packing (see Supporting Information Figure S5).

The solid-state study on the complexation of calcium cations with host **1** demonstrated that 1:2 complexation of **1** to cations is indeed possible. Analogous to the anion-binding study, ^1H NMR titration experiments were performed on several alkali metal and alkaline earth metal cations as perchlorate salts ($NaClO_4$, $Mg(ClO_4)_2$, and $Ca(ClO_4)_2$) or hexafluorophosphate salt (KPF_6) in the same solvent mixtures used for the anion binding studies shown above. The KPF_6 was chosen instead of $KClO_4$ as the latter is not soluble enough in any of the solvent mixtures used in this study.

In DMSO-d_6/acetone-d_6 (1:9, v/v), the titration of **1** with all of the cation salts tested did not induce any significant resonance shift. This is evidence of extremely weak binding (K_1 and K_2 < 1 M^{-1}) or no cation binding toward **1** is due to the strong electron-donating effect of the solvent mixture competing in the binding of cation (see Supporting Information Figure S27). On the contrary, titration experiments performed with the less competitive solvent mixtures resulted in downfield shifts for the resonances of the ethyleneoxy protons (−OCH_2CH_2−). This is due to the cation binding toward the electron-donating oxygen atoms on the "crown-6" motif of **1**, consequently deshielding the ethyleneoxy protons via an inductive effect. More interestingly, the binding of cations also induced significant shifts in the resonances of the amide-H and all of the aromatic-H signals as shown in Figure 4, demonstrating the complexity and different binding mechanisms of alkali metals and alkaline earth metal cations towards **1**.

The ^1H NMR titration of **1** with $Ca(ClO_4)_2$ in $CDCl_3$/CD_3CN (1:9, v/v, Figure 4a) and in $CDCl_3$/CD_3CN (1:1, v/v, Figure 4b) both resulted in almost identical $\Delta\delta$ curves for all of the proton signals. The downfield shift in the resonance of amide-H (deshielded due to inductive effect) suggests that the carbonyl oxygen atoms are directed toward the complexation of Ca^{2+}, as supported by the single-crystal X-ray analysis of **1**·2[$Ca(ClO_4)_2$] complex. The shifts in the resonance of all of the aromatic-H signals are likely due to the structural reorganization and change in the conformation of **1** during the binding toward Ca^{2+}.

The prominent "dip" in the $\Delta\delta$ curve of aromatic-H4 at 1 equiv of $Ca(ClO_4)_2$, followed by the "plateau" of all of the proton signals at 2 equiv, demonstrates the strong binding of two Ca^{2+} in these two solvent mixtures. In addition, progressive exchange-broadening of aromatic-H1 and H4 signals on the NMR time scale was observed upon titration until saturation at 2 equiv of $Ca(ClO_4)_2$ (see Supporting Information Figures S15, S19 and S22). Fortunately, these are not true slow exchange processes, therefore allowing centroid peak-picking on the broad signals for the average equilibrium between free host (**1**), H:G (**1**·Ca^{2+}), and H:G_2 (**1**·2Ca^{2+}) complexes.

Inspection of the ^1H NMR data from the titration of **1** with $Mg(ClO_4)_2$ in $CDCl_3$/CD_3CN (1:9, v/v, Figure 4d) and $CDCl_3$/CD_3CN (1:1, v/v, Figure 4e) also clearly shows a 1:2 equilibria as evident by inspection of the aromatic H1 and to a lesser degree, the amide-H binding isotherms. In the more polar $CDCl_3$/CD_3OD (9:1, v/v, Figure 4f), however, upon the addition of $Mg(ClO_4)_2$, the shifts in host **1** are so small that binding must either be very weak (K_1 and K_2 < 1 M^{-1}) or no binding is taking place at all.

dx.doi.org/10.1021/ja503383e | J. Am. Chem. Soc. 2014, 136, 7505−7516

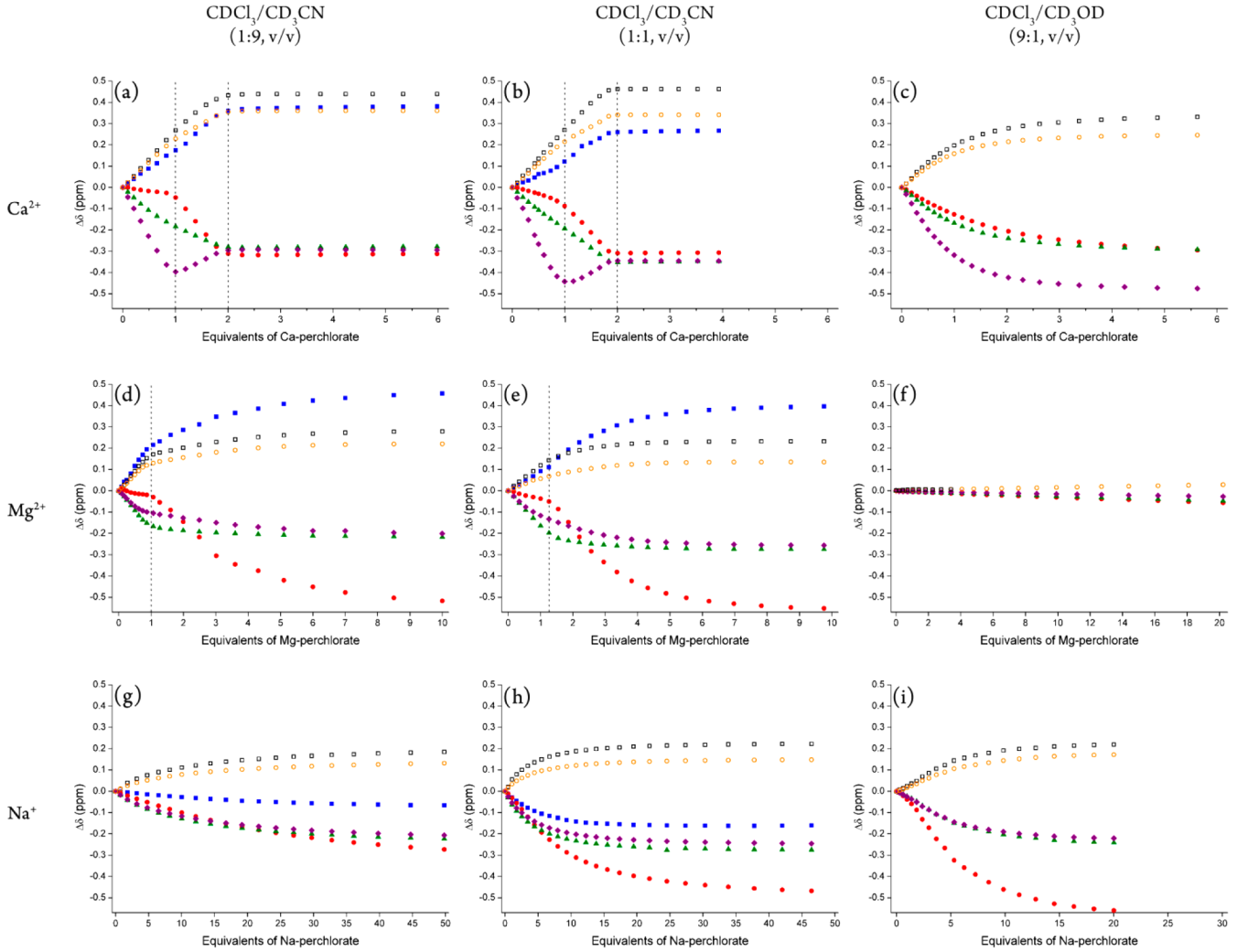

Figure 4. Plots of ^{1}H NMR titrations (400 MHz, 298 K) of host **1** (1.0 mM) with perchlorate cation salts ($Ca(ClO_4)_2$, $Mg(ClO_4)_2$ and $NaClO_4$), showing the change in chemical shifts ($\Delta\delta$) for ethylene-Hd (□), ethylene-He (yellow ○), amide-H (blue ■), aromatic-H1 (red ●), aromatic-H3 (green ▲), and aromatic-H4 (purple ◆) in three different solvent mixtures, $CDCl_3/CD_3CN$ (1:9, v/v), $CDCl_3/CD_3CN$ (1:1, v/v), and $CDCl_3/CD_3OD$ (9:1, v/v). Amide-H is undetectable in $CDCl_3/CD_3OD$ (9:1, v/v) due to hydrogen−deuterium exchange with CD_3OD. Points of ethylene-Hd are not reported in plot (f) at the higher equivalents region due to overlapping signals with the H_2O peak. *y*-axes ($\Delta\delta$) for all nine plots are in the same range for comparison. In plots (a,b, d,e), vertical dotted lines demark the apparent main inflection points (dips and kinks) on the binding isotherms.

The binding of $NaClO_4$ to **1** is more complicated, and visual inspection of the binding isotherms in $CDCl_3/CD_3CN$ (1:9, v/v, Figure 4g) and $CDCl_3/CD_3CN$ (1:1, v/v, Figure 4h) does not immediately suggest or rule out a 1:1 or 1:2 equilibria. Interestingly, in the more polar $CDCl_3/CD_3OD$ (9:1, v/v, Figure 4i), the binding appears quite strong, and the binding isotherm for the aromatic-H1 shows a clear sigmoidal shape, suggesting a more complex equilibria than 1:1.

With enough solid-state and solution evidence to suggest that 1:2 equilibria could play a major role in the binding of cations to **1**, the data were now analyzed with respect to the different 1:1 and 1:2 models discussed above (Table 1). Data from the titration of host **1** with the three aforementioned cation salts were analyzed; $Ca(ClO_4)_2$, $NaClO_4$, and $Mg(ClO_4)_2$ in the $CDCl_3/CD_3CN$ (1:9, v/v), $CDCl_3/CD_3CN$ (1:1, v/v) and $CDCl_3/CD_3OD$ (9:1, v/v) solvent mixtures were used, with the exception of the nonbinding $Mg(ClO_4)_2$ in $CDCl_3/CD_3OD$ (9:1, v/v). Three or four repeats of these ^{1}H NMR titrations of **1** focused on the shifts in the resonances of ethylene-Hd, ethylene-He, aromatic-H3, and aromatic-H4. The data were fitted to both the 1:1 model and the four variants of the 1:2 models shown in Table 1 (see the Supporting Information for a detailed description). In the case of the $NaClO_4$ binding to **1** in $CDCl_3/CD_3OD$ (9:1, v/v), the data were also fitted to the full 2:1 model to seek an explanation of the observed sigmoidal binding isotherms mentioned above (Figure 4i). Additionally, the binding of the KPF_6 salt to **1** in $CDCl_3/CD_3CN$ (1:9, v/v) was analyzed in the same manner. For solubility reasons, it was not possible to investigate the binding of KPF_6 to **1** in $CDCl_3/CD_3CN$ (1:1, v/v) and $CDCl_3/CD_3OD$ (9:1, v/v).

Comparing the fits and number of parameters (see Supporting Information Tables S12−S20 and Figures S15−S23) indicated as shown in Table 3 that only the full 1:2 and noncooperative 1:2 models needed to be considered for cation binding to **1**, the only exception being $NaClO_4$ binding to **1** in $CDCl_3/CD_3OD$ (9:1, v/v) where the full 2:1 model might also play a role.

dx.doi.org/10.1021/ja503383e | J. Am. Chem. Soc. 2014, 136, 7505−7516

Table 3. Most Plausible Binding Models, Stepwise K_1 and K_2 Association Constants, and Interaction Parameters (α) for the Complexation of Host 1 toward Various Cation Salts Obtained from ^{1}H NMR Titrations (400 MHz) at 298 K in the Solvent Mixtures Shown[a]

cation salt	solvent	binding model[b]	K_1 (M^{-1})	K_2 (M^{-1})	α[c]
$Ca(ClO_4)_2$	$CDCl_3/CD_3CN$ (1:9, v/v)[d]	full 1:2	>1 × 10^6[e]	>1 × 10^6[e]	N/A
	$CDCl_3/CD_3CN$ (1:9, v/v)[d]	noncooperative 1:2	>1 × 10^6[e]	>1 × 10^6[e]	N/A
	$CDCl_3/CD_3CN$ (1:1, v/v)	full 1:2	>1 × 10^6[e]	>1 × 10^6[e]	N/A
	$CDCl_3/CD_3CN$ (1:1, v/v)	noncooperative 1:2	>1 × 10^6[e]	>1 × 10^6[e]	N/A
	$CDCl_3/CD_3OH$ (9:1, v/v)	full 1:2	6600 (1800)	480 (140)	0.29
	$CDCl_3/CD_3OH$ (9:1, v/v)	noncooperative 1:2	4300 (500)[f]	1075 (130)[f]	1.0[f]
$NaClO_4$	$CDCl_3/CD_3CN$ (1:9, v/v)	full 1:2	6100 (9000)	72.0 (7.1)	0.05
	$CDCl_3/CD_3CN$ (1:9, v/v)	additive 1:2	276 (52)	42 (7.1)	0.61
	$CDCl_3/CD_3CN$ (1:9, v/v)	noncooperative 1:2	200 (13)[f]	50 (3.2)[f]	1.0[f]
	$CDCl_3/CD_3CN$ (1:1, v/v)	full 1:2	280 (40)	23.8 (8.7)	0.34
	$CDCl_3/CD_3CN$ (1:1, v/v)	noncooperative 1:2	500 (240)[f]	125 (60)[f]	1.0[f]
	$CDCl_3/CD_3OH$ (9:1, v/v)	full 1:2	220 (40)	380 (60)	6.3
	$CDCl_3/CD_3OH$ (9:1, v/v)	full 2:1[g]	350 (33)[g]	negative[g]	N/A
	$CDCl_3/CD_3OH$ (9:1, v/v)	noncooperative 1:2	4300 (500)[f]	1075 (130)[f]	1.0[f]
$Mg(ClO_4)_2$	$CDCl_3/CD_3CN$ (1:9, v/v)	full 1:2	56 000 (32 000)	170 (59)	0.01
	$CDCl_3/CD_3CN$ (1:1, v/v)	full 1:2	4300 (510)	880 (200)	0.82
	$CDCl_3/CD_3CN$ (1:1, v/v)	noncooperative 1:2	3500 (770)[f]	875 (190)[f]	1.0[f]
KPF_6	$CDCl_3/CD_3CN$ (1:9, v/v)	full 1:2	68.9 (1.7)	2.9 (2.0)	0.17

[a]The data here are a summary of a more detailed analysis of binding data shown in Supporting Information Tables S12−S20 and Figures S15−S23, and only data for the binding model(s) that fitted best with the experimental data are shown here (see above and the Supporting Information for more details). Unless indicated otherwise, the numbers shown are the rounded averages from triplicate measurements with the standard deviation shown in brackets. [b]See Table 1 and the Supporting Information for details on the difference between these binding models and how the best model(s) are selected. [c]The interaction parameter $\alpha = 4K_2/K_1$ with $\alpha > 1$ indicating positive cooperativity, $\alpha < 1$ negative cooperativity, and $\alpha = 1$ no cooperativity.[6a−c] [d]This titration study was repeated four times. [e]The raw calculated binding constants were well in excess of 10^6 M^{-1}, which is usually considered the upper limit of binding constants that can be reliably obtained from ^{1}H NMR titration studies.[6c,d,19] [f]For the noncooperative 1:2, the ratio of K_1 and K_2 is by definition fixed as $K_1 = 4K_2$ and hence $\alpha = 1$. [g]The data from the 2:1 model are included here as it gives a reasonable fit; however, as the fitting process gave a nonrealistic negative value for K_2 (possibly as 2:1 complex would only be detectable over a narrow range within the titration), the K_1 value reported here needs to be interpreted with caution.

The results in Table 3 suggest that the overall trends for cation binding to **1** are more complicated than the corresponding study of anion binding to **1** (Table 2). However, it is clear that in all cases the 1:2 binding model prevails, confirming the effective ditopic nature of **1** when it comes to the binding of cations. Interestingly, cations appear to bind to **1** in either noncooperative or relatively weak negatively cooperative fashion. In these cases, even when the full 1:2 model is used, the interaction parameter α is, with few notable exceptions, in the range of 0.3−0.8. On the basis of electrostatic repulsion alone, negative cooperativity would be expected for the 1:2 binding of cations to **1**, but the results here suggest that this repulsion does not play a major role, possibly as the two cation binding sites are quite far apart as evident in the solid-state structure of the **1**·2[$Ca(ClO_4)_2$] complex in Figure 3b with the $Ca^{2+}\cdots Ca^{2+}$ distance of 10.337 Å.

When looking more closely at the results for the binding of monovalent alkali metal cations, it can be seen that $NaClO_4$ binds more strongly than KPF_6 in $CDCl_3/CD_3CN$ (1:9, v/v), but potassium in particular does so with considerable negative cooperativity ($\alpha < 0.2$). One possible explanation is that these cations could bind in a different manner to **1** than the solid-state structure of the **1**·2[$Ca(ClO_4)_2$] complex would suggest. Comparison of the binding isotherms for the amide-H upon binding to $NaClO_4$ (Figure 5g−i) with $Ca(ClO_4)_2$ (Figure 5a−c) and $Mg(ClO_4)_2$ (Figure 5d−f) also suggests that they might bind differently, but in the absence of solid-state evidence it is difficult to ascertain this hypothesis.

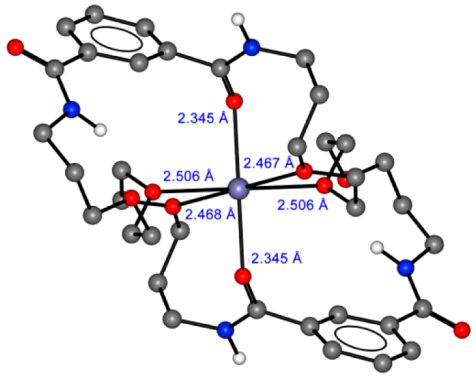

Figure 5. DFT (PBE1PBE/6-31+G(d)) optimized structure of **1**·Ca^{2+} complex without counterions; all H atoms are omitted for clarity, except amide-H.

As was already mentioned, the binding of $NaClO_4$ to **1** in $CDCl_3/CD_3OD$ (9:1, v/v) appears to be quite complex. Comparison of the different binding models used to fit these data showed three reasonably plausible options: the full 2:1, the full 1:2, and the noncooperative 1:2 models. In the case of the 2:1 model, the K_2 could not be reliably determined, but this could be explained on the grounds that the corresponding 2:1·**1**$_2Na^+$ complex might be difficult to detect. On the other hand, the full 1:2 model suggests positive cooperativity (α = 6.30), but this might be because the data are skewed due to an underlying competing formation of a 2:1 complex. The most

dx.doi.org/10.1021/ja503383e | J. Am. Chem. Soc. 2014, 136, 7505−7516

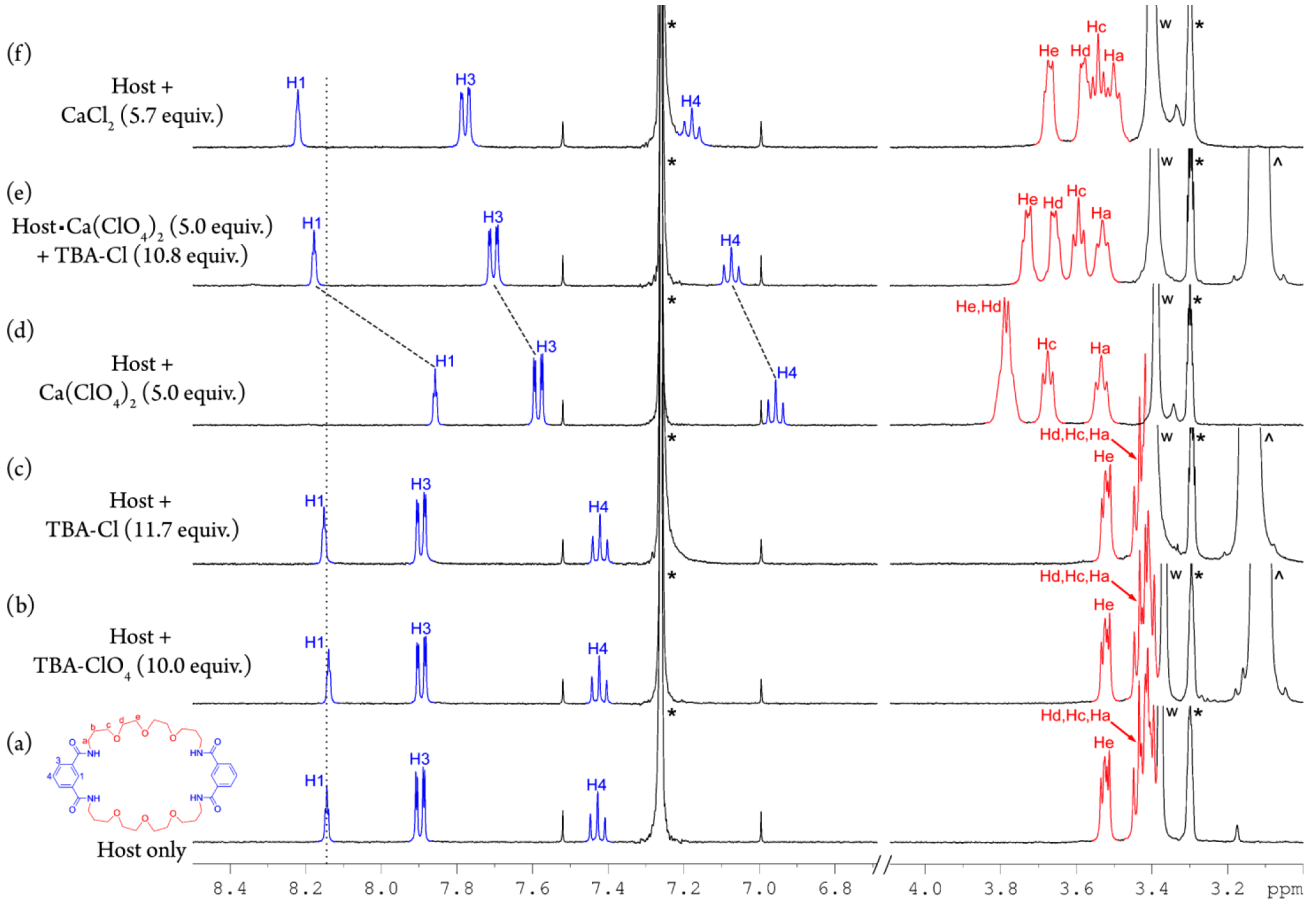

Figure 6. Partial ^{1}H NMR spectra (400 MHz, 298 K) in $CD_3OD/CDCl_3$ (1:9, v/v) of (a) host **1** (1.0 mM), (b) **1** titrated with TBA-ClO_4 (10.0 equiv), (c) **1** titrated with TBA-Cl (11.7 equiv), (d) **1** titrated with $Ca(ClO_4)_2$ (5.0 equiv), (e) **1** in the presence of $Ca(ClO_4)_2$ (5.0 equiv) titrated with TBA-Cl (10.8 equiv), and (f) **1** titrated with $CaCl_2$ (5.7 equiv). Vertical dotted line demarking the original chemical shift of aromatic-H1 and dashed lines show shifts upon titration of TBA-Cl in the presence of $Ca(ClO_4)_2$. "*", "w", and "∧" denote peaks of NMR solvents, water, and TBA^+ cation, respectively.

plausible scenario is therefore that upon adding $NaClO_4$ to **1** in $CDCl_3/CD_3OD$ (9:1, v/v), a 2:1 complex is formed first, followed by the formation of a 1:1 complex and ultimately a 1:2 complex once enough excess $NaClO_4$ is present. Such a 2:1−1:1−1:2 progression has been previously reported for cyclodextrins.[20] It is also noteworthy that the nature of the solvent mixture does not seem to have a very strong effect on the binding strength of $NaClO_4$ to **1**.

The data for the divalent $Mg(ClO_4)_2$ and $Ca(ClO_4)_2$ do however show a strong correlation with the polarity of the solvent. For both of the $CDCl_3/CD_3CN$ mixtures, the binding of $Ca(ClO_4)_2$ is too strong to be accurately determined as it has been shown previously that ^{1}H NMR titration data cannot be used to measure binding constants above 10^6 M^{-1}.[6c,d,19] In the more competitive $CDCl_3/CD_3OD$ (9:1, v/v) solvent, the binding of $Ca(ClO_4)_2$ appears to be mildly negatively cooperative or noncooperative; the difference between these two binding models is not considerable, although the full 1:2 model with α = 0.29 appears to be slightly better (see Supporting Information Table S19). As mentioned previously, $Mg(ClO_4)_2$ does not appear to bind to **1** in the $CDCl_3/CD_3OD$ (9:1, v/v) solvent system (Figure 4f), while the data from Table 3 suggests the binding of $Mg(ClO_4)_2$ to **1** is considerably weaker in $CDCl_3/CD_3CN$ (1:1, v/v) than in $CDCl_3/CD_3CN$ (1:9, v/v). Interestingly, the binding is strongly negatively cooperative (α = 0.01) in the latter, less protic (1:9, v/v) system while noncooperative ($\alpha \approx 0.8-1$) in the more protic $CDCl_3/CD_3CN$ (1:1, v/v) mixture.

The NMR titration data for $Ca(ClO_4)_2$ do feature prominent "dips" and "kinks" in some of the binding isotherms (Figure 4a,b), suggesting the existence of two very distinct conformations for the **1**·Ca^{2+} and **1**·2Ca^{2+} complexes. With both single-crystal X-ray structures of the free host **1** and the **1**·2[$Ca(ClO_4)_2$] complex available, we carried out two-dimensional NOESY experiments to elucidate some structural information about the 1:1 **1**·$Ca(ClO_4)_2$ complex and probe the conformational changes from the free host **1** to the 1:1 and then 1:2 complex between **1** and $Ca(ClO_4)_2$ (see the Supporting Information for details). These NOESY experiments were carried out in $CDCl_3/CD_3OD$ (9:1, v/v) at 298 K. In the free host **1**, the intramolecular NOE cross-peaks (see Supporting Information Figure S29) between aromatic-H1 with H4, and all aromatic-H with the distal ethylene-Hd and He signals, indicate the folded-closed conformation of the macrocycle that is consistent with the single-crystal X-ray analysis of **1**.

Upon the addition of 1 equiv of $Ca(ClO_4)_2$ to **1**, the data for the full 1:2 model in Table 3 allow an estimation of the distribution of the free host **1**, the **1**·Ca^{2+}, and the **1**·2Ca^{2+} complex as 38%, 58%, and 7% (see the Supporting Information for details). At this point, all of the NOE contacts between the aromatic H4 and the ethylene protons are gone (see

dx.doi.org/10.1021/ja503383e | J. Am. Chem. Soc. 2014, 136, 7505−7516

Table 4. Most Plausible Binding Models, Stepwise K_1 and K_2, and Overall β_{12} Association Constants, Interaction Parameters (α), and Relative Quality of Fit for the Complexation of Host 1 toward Calcium Chloride Salt Combination Obtained from ^{1}H NMR Titrations (400 MHz) at 298 K in $CD_3OD/CDCl_3$ (1:9, v/v)[a]

salt added	binding model[b]	K_1 (M^{-1})	K_2 (M^{-1})	β_{12} (M^{-2})[c]	α[d]	cov_{fit} factor[e]
$CaCl_2$	noncooperative 1:2	200 (60)[f]	50 (16)[f]	10 000 (6700)	1.0[f]	18
	full 1:2	210 (45)	50 (9)	10 500 (2600)	0.95	23
TBA-Cl	noncooperative 1:2	450 (62)[f]	110 (15)[f]	50 000 (13 000)	1.0[f]	3.4
+5 equiv	full 1:2	<0.1[g]	>10[6g]	13 400 (2200)	N/A	9.2
$Ca(ClO_4)_2$	additive 1:2	9 (4)	3400 (2600)	24 000 (3900)	1500	1.4

[a]The data here are a summary of a more detailed analysis of binding data shown in Supporting Information Tables S21−S22 and Figures S24−S25, and only data for the binding model(s) that fitted best with the experimental data are shown here (see above and the Supporting Information for more details). The numbers shown are the rounded averages from four repeat measurements with the standard deviation shown in brackets. [b]See Table 1 and the Supporting Information for details on the difference between these binding models and how the best model(s) are selected. [c]The overall association constant $\beta_{12} = K_1 \times K_2$. [d]The interaction parameter $\alpha = 4K_2/K_1$ with $\alpha > 1$ indicating positive cooperativity, $\alpha < 1$ negative cooperativity, and $\alpha = 1$ no cooperativity.[6a−c] [e]The relative quality of fit; cov_{fit} factor = cov_{fit} for the 1:1 model divided by the cov_{fit} for the binding model under study, where cov_{fit} is the (co)variance of the residuals divided by the (co)variance of the raw data.[6c] [f]For the noncooperative 1:2, the ratio of K_1 and K_2 is by definition fixed as $K_1 = 4K_2$ and hence $\alpha = 1$. [g]The calculated stepwise binding constants were either much smaller than 1 or well in excess of 10^6 M^{-1}; however, as explained in the text, the overall association constant β_{12} was within a reasonable range for what can be reliably obtained from ^{1}H NMR titration studies.[6c,d,19]

Supporting Information Figure S30). Proceeding to 2 (see Supporting Information Figure S31) and finally 5 equiv of $Ca(ClO_4)_2$, the remaining NOE cross peaks between the aromatic H1 and the ethylene protons also disappear (see Supporting Information Figure S32), at which point the calculated ratios of free **1**, **1**·Ca^{2+}, and **1**·2Ca^{2+} are 2%, 39%, and 59%, respectively.

This progression of NOE cross peaks is consistent with a model whereby the first binding of $Ca(ClO_4)_2$ to **1** opens the folded-closed conformation. We postulated that the first Ca^{2+} was more likely to interact with both parts of the crown-6 system, rather than binding to one side only as this would probably lead to symmetry breakdown in the ^{1}H NMR, which was not observed. To this end, a computational optimization study was carried out on a structure that was created by docking Ca^{2+} in the center of the single-crystal X-ray structure of the free host **1**. This structure was then first minimized using an MM2 force field with six dummy bonds between the Ca^{2+} and the crown-6 oxygen atoms. The dummy bonds were then removed and the full structure optimized using DFT (PBE1PBE/6-31+G*) theory (see the Supporting Information for details), which yielded the structure of the **1**·Ca^{2+} complex shown in Figure 5. This study suggests that the complexation of one Ca^{2+} to **1** could result in a 6-coordinated quasi-octahedral geometry with archetypal $Ca^{2+}\cdots O$ distances (2.345−2.506 Å), with two of the isophthalamide carbonyl groups coordinated to Ca^{2+} together with four of the crown-6 oxygen atoms.

Allosterically Controlled Switching "On" of Anion Binding. The above ^{1}H NMR titration studies and single-crystal X-ray structure studies have conclusively shown that host **1** is indeed capable of binding two anions and two cations at four distinctly different binding sites. In other words, the host **1** appears to be a tetratopic ion-pair receptor. To investigate the ion-pair binding capabilities of **1**, we decided to focus our attention on the binding of the Ca^{2+} and Cl^- ions to **1**.

We were particularly intrigued to see if the binding of Ca^{2+} to **1** could cooperatively enhance the binding of Cl^- by a combination of favorable electrostatic interactions and the ability of Ca^{2+} to open the folded-closed conformation of the free host **1** as discussed in the previous section. To this end, we choose to conduct these studies in the $CDCl_3/CD_3OD$ (9:1, v/v) solvent system; however, TBA-Cl and TBA-ClO_4 did not appear to bind to **1** with any measurable affinity as evident by comparison to the spectra of the free host **1** (Figure 6a) with over 10 equiv of TBA-ClO_4 (Figure 6b) and TBA-Cl (Figure 6c).

As previously mentioned, the calculated ratios of free **1**, **1**·Ca^{2+}, and **1**·2Ca^{2+} are 2%, 39%, and 59% in the presence of 5 equiv of $Ca(ClO_4)_2$ in the $CDCl_3/CD_3OD$ (9:1, v/v), corresponding to 98% of **1** being bound to Ca^{2+}. We chose these conditions as a starting point for a ^{1}H NMR titration with TBA-Cl in the presence of $Ca(ClO_4)_2$. While keeping the concentration of **1** (1.0 mM) and $Ca(ClO_4)_2$ (5.0 mM) constant (Figure 6d), the titration with 10 equiv of TBA-Cl induced a very notable downfield shift of aromatic-H1 in the NMR spectrum (Figure 6e), indicative of strong Cl^- binding.

Encouraged by these results, the ion-pair binding properties of **1** were probed by the addition of 5 equiv of $CaCl_2$ to **1**. The resulting ^{1}H NMR spectra (Figure 6f) shows both a downfield shift of the aromatic-H1 and all of the ethylene-H signals, demonstrating simultaneous binding of both the anion (Cl^-) and the cation (Ca^{2+}) to the ion-pair receptor **1**. As evident by comparing Figure 6e and f, the NMR spectra of [**1** + $Ca(ClO_4)_2$ (5.0 equiv) + TBA-Cl (10.8 equiv)] and [**1** + $CaCl_2$ (5.7 equiv)] are remarkably similar in both the isophthalamide aromatic region (anion binding site) and the crown-6 region (cation binding site). Importantly, these results clearly represent the binding of Cl^- within the two clefts of the isophthalamide moieties of **1**, while Ca^{2+} remains bound to the two "half-crown/two carbonyl" cation binding sites, illustrating the tetratopic nature of the ion-pair host **1**.

It should be stressed that the underlying equilibria are almost certainly more complex than a stepwise 1:2 complex formation. The tetratopic nature of **1** suggests it binds two Ca^{2+} and two Cl^- anions; yet the addition of two $CaCl_2$ to **1** would yield two bound Ca^{2+}, two bound Cl^-, and two unbound (or outer sphere) Cl^-. Likewise, in the presence of 5 equiv of $Ca(ClO_4)_2$, our calculations above would suggest a 2:3 ratio in the formation of the 1:1 and 1:2 complexes between Ca^{2+} and **1**. This ratio would almost certainly change as Cl^- is added to this system. Taking this all into account, the fit between the experimental data and some of the binding models used is surprisingly good (see Supporting Information Tables S21, S22 and Figures S24, S25).

The results shown in Figure 6 suggest that the binding of Cl^- in $CDCl_3/CD_3OD$ (9:1, v/v) can be switched "on" in the

dx.doi.org/10.1021/ja503383e | J. Am. Chem. Soc. 2014, 136, 7505−7516

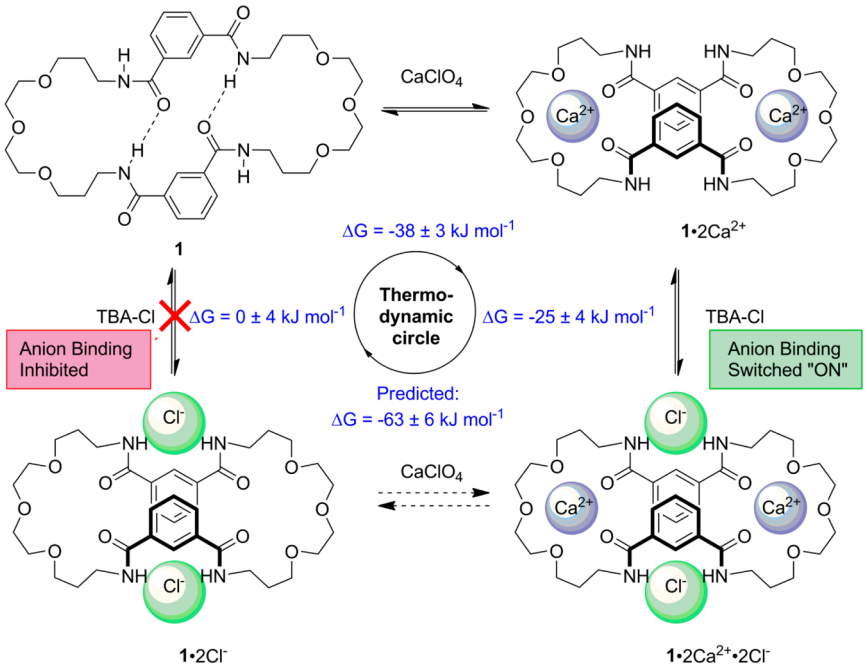

Figure 7. Overall thermodynamic binding circle[4g] involving $CaClO_4$ and TBA-Cl binding to host **1** in $CDCl_3/CD_3OD$ (9:1, v/v). Shown in blue are the experimental determined from ^1H NMR titration (400 MHz, 298 K) (top, left and right of circle) and estimated (bottom of circle) binding free energies (ΔG) with errors corresponding to the expanded uncertainty at 95% confidence level. The postulated conformations of **1** at different stages in this binding circle are also shown schematically. Dotted equilibria arrows indicate a hypothetical equilibria (not measured). For full details, see discussion in the text.

presence of Ca^{2+}. To investigate the stoichiometry and strength of these interactions further, titration studies (four repeats) on **1** in $CDCl_3/CD_3OD$ (9:1, v/v) were carried out using (i) $CaCl_2$ and (ii) TBA-chloride with 5 equiv of $Ca(ClO_4)_2$ present. As in the case of the anion and cation studies above, the data were then fitted to the 1:1 binding model and all four variants of the 1:2 binding model shown in Table 1 (see the Supporting Information for details and Tables S21, S22 and Figures S24, S25) with the results summarized in Table 4.

The summary in Table 4 suggests that the full 1:2 and noncooperative 1:2 models are probably the most suitable models to describe both the $CaCl_2$ and the TBA-Cl with 5 equiv of $Ca(ClO_4)_2$ titrations of **1**. In the latter case, we also included the less suitable additive 1:2 model to try and give a better estimation on the stepwise 1:1 and 1:2 binding constants in the full 1:2 model. This was done as the stepwise binding constants were unrealistically high and low in this case. However, the product of these, the overall binding constant β_{12} ($=K_1 \times K_2$), fitted well with the other model, and all of the other indicators suggested that the full 1:2 model was plausible.

From the data in Table 4, it appears quite clear that the binding of $CaCl_2$ is noncooperative ($\alpha \approx 1$) with stepwise $K_1 \approx 200\ M^{-1}$ and $K_2 \approx 50\ M^{-1}$ corresponding to $\beta_{12} = 10\,000\ M^{-2}$, and the differences between the full 1:2 and noncooperative 1:2 model are negligible. For the TBA-Cl with 5 equiv of $Ca(ClO_4)_2$ titrations, the results from the full 1:2 and additive 1:2 models indicate very strong positive cooperativity ($\alpha >$ 1000), while the noncooperative 1:2 suggests otherwise ($\alpha =$ 1). Interestingly, all three models give overall association constants β_{12} that are within the same order of magnitude ($\beta_{12} \approx 10\,000{-}50\,000\ M^{-2}$).

Comparing the binding isotherms for the $CaCl_2$ (see Supporting Information Figure S24) and TBA-Cl with 5 equiv of $Ca(ClO_4)_2$ (see Supporting Information Figure S25) titrations, the two appear qualitatively different, with the former showing a typical hyperbolic shape while the latter was an unusual sigmoidal shape. A sigmoidal binding isotherm is often a signature of positive cooperativity, such as in oxygen binding to hemoglobin.[2a,c,e] For this reason, the positive cooperativitity full 1:2 and additive 1:2 models in Table 4 appear to describe better the binding of TBA-Cl to **1** in the presence of 5 equiv of $Ca(ClO_4)_2$.

Taken together, these results demonstrate not only that **1** is a tetratopic ion-pair receptor but that addition of Ca^{2+} to **1** cooperatively switches "on" anion binding in **1** in a solvent that otherwise is too competitive for any anion binding to be observed. This switching "on" can be partially explained by favorable electrostatic interactions between the bound cation(s) in **1** and the added anions. However, the very significant conformational changes that **1** undergoes upon binding to Ca^{2+} from a folded-closed to an open conformer do undoubtedly also play a significant role in switching "on" Cl^- binding in $CDCl_3/CD_3OD$ (9:1, v/v). We therefore conclude that the switching "on" is also allosteric in nature[5a,c,21] and that it represents a case of strong positive heterotropic allosterism.[4c,d]

The success of switching "on" of Cl^- recognition with **1** in the presence of Ca^{2+} prompted us to investigate the binding of Ca^{2+} in the presence of Cl^-. Because of the extremely weak or nonexisting binding of Cl^- to **1** in $CDCl_3/CD_3OD$ (9:1, v/v), the addition of 100 equiv of TBA-Cl could only induce a very small shift in the ^1H NMR spectra, which could not be reliably fitted to any binding model. Yet even with a very optimistic $K_1 = 5\ M^{-1}$, only ~12% of **1** would be bound to Cl^- in a 1:1 complex in the presence of 20 equiv of Cl^-. Regardless, this solution was then titrated with $Ca(ClO_4)_2$.

The resulting binding isotherms (see Supporting Information Figure S28) for the addition of $Ca(ClO_4)_2$ to **1** in the presence of 20 equiv of TBA-Cl are qualitatively quite different from

dx.doi.org/10.1021/ja503383e | J. Am. Chem. Soc. 2014, 136, 7505−7516

those obtained for $Ca(ClO_4)_2$ in the absence of TBA-Cl (Figure 4c). Attempts to fit the data to any of the binding models in Table 1 were unsuccessful. The most likely explanation for this and the multiple inflection points seen in these isotherms is that the initial addition of Ca^{2+} enhances the Cl^- binding, which in turn enhances Ca^{2+} binding in a nonlinear fashion. Without the ability to reach close to 100% saturation of **1** with Cl^- in $CDCl_3/CD_3OD$ (9:1, v/v) prior to the addition of $Ca(ClO_4)_2$, quantification of the binding of the latter in the presence of Cl^- remains elusive.

Although we were not able to measure the binding constant of Ca^{2+} to **1** in the presence of Cl^-, we can estimate it by analyzing the thermodynamic binding circle for the equilibria between **1**, Ca^{2+}, and Cl^- (Figure 7).[4g] By assuming that the binding free energy (ΔG) for Cl^- to **1** in $CDCl_3/CD_3OD$ (9:1, v/v) is $\Delta G \approx 0$ kJ mol^{-1}, we arrive at a $\Delta G = -63 \pm 6$ kJ mol^{-1} for the addition of $Ca(ClO_4)_2$ to **1** in the presence of 2 equiv of Cl^-. This would translate to $\beta_{12} \approx 1.1 \times 10^{11}$ M^{-2} or $K_1 \approx 6.5 \times 10^5$ M^{-1} and $K_2 = 1.6 \times 10^5$ M^{-1} if the binding was noncooperative.

CONCLUSIONS

We have shown here that the macrocycle **1** is a tetratopic ion-pair host that displays a rich collection of cooperative binding properties. To analyze the binding properties of **1**, we used a combination of single-crystal X-ray analysis, computational studies, but most importantly, a detailed comparison of triplicate (or more) ^{1}H NMR titration data analyzed by at least five different binding models (Table 1). We believe this is the first time such a systematic approach has been used to analyze cooperative binding, but that the results here demonstrate the generic utility of this approach when analyzing complex binding data.

Our analysis of the ^{1}H NMR titration data for **1** showed that as a ditopic anion host, **1** shows fairly strong negative cooperativity (α between 0.01−0.05) for the strongly binding Cl^- and OAc^- in nonprotic solvents, which is then somewhat attenuated ($\alpha > 0.2$) in more competitive solvents and for weaker binding anions such as Br^-, I^-, and NO_3^-. For cation binding, the results were more variable depending both on the cation and on the nature of the solvent, but in the majority of cases, negative cooperative binding appeared to prevail. More importantly, single-crystal X-ray analysis of the **1**·2[$Ca(ClO_4)_2$] complex revealed two distinct unusual "half-crown/two carbonyl" cation binding sites more than 10 Å apart. Comparison of this structure with the one obtained for the free host **1**, computational studies, and NOESY ^{1}H NMR analysis showed that the binding of two Ca^{2+} to **1** leads to a change from a folded-closed to an open confirmation of **1**, possibly via a 6-coordinated quasi-octahedral 1:1 **1**·[$Ca(ClO_4)_2$] complex involving two of the four isophthalamide carbonyl groups.

Using a competitive solvent system ($CDCl_3/CD_3OD$ (9:1, v/v)) where Cl^- binding to **1** was practically nonexistent, we were then able to show that the prior addition of Ca^{2+} allowed us to switch "on" anion binding in **1** despite the very competitive nature of the $CDCl_3/CD_3OD$ (9:1, v/v) solvent system. Interestingly, the data also suggested that after switching Cl^- binding "on" with Ca^{2+}, the two Cl^- bound either noncooperatively or with strong positive cooperativity, partly evident by the sigmoidal binding isotherms observed for the addition of TBA-Cl to a mixture of **1** with 5 equiv of $Ca(ClO_4)_2$. The results here also show that Ca^{2+} and Cl^- can both be added sequentially as $Ca(ClO_4)_2$, followed by TBA-Cl, or simultaneously by adding $CaCl_2$ to the tetratopic ion-pair host **1**. Although we were not able to measure the binding strength of Ca^{2+} in the presence of Cl^-, the thermodynamic binding cycle[4g] suggested that the free energy enhancement ($\Delta\Delta G$) for Ca^{2+} binding to **1** could be as much as −25 kJ mol^{-1} as compared to Ca^{2+} binding to **1** in the absence of Cl^-.

Finally, it is worth noting that the cation-induced switching "on" of anion binding in **1** appears to be allosteric in nature. This is evident by the conformational changes that **1** undergoes upon binding Ca^{2+}, which preorganizes the host **1** toward binding to the Cl^- anion. Interestingly, this also appears to turn off or even reverse the negative cooperativity between the first and second Cl^- binding to **1**. Taken together, the results of this work demonstrate how the relatively simple tetratopic ion-receptor **1** can allow us to study complex cooperative interactions at the fundamental level. This mimicking of complex cooperative systems in nature will also ultimately allow us to design better cooperative synthetic supramolecular systems for information transfer and catalysis.

ASSOCIATED CONTENT

Supporting Information

Crystallographic (CIF), experimental procedures, spectra of **1**, details on single-crystal X-ray analysis, details on methodology for binding studies, selected spectra from binding studies, all binding isotherms and calculated binding constants, details on computational and two-dimensional, along with supporting figures. This material is available free of charge via the Internet at http://pubs.acs.org.

AUTHOR INFORMATION

Corresponding Author

p.thordarson@unsw.edu.au

Notes

The authors declare no competing financial interest.

ACKNOWLEDGMENTS

We would like to thank the Mark Wainwright Analytical Centre (UNSW) for access to instruments, and we thank Dr. Tom Caradoc-Davies (Australian Synchrotron) for assistance. We acknowledge the Australian Research Council for Discovery Project Grant (DP130101512) and a Future Fellowship to P.T. (FT120100101) and the Australian Government and University of New South Wales for an EIPRS Ph.D. scholarship to E.N.W.H.

REFERENCES

(1) (a) Whitty, A. *Nat. Chem. Biol.* **2008**, *4*, 435. (b) Bai, F.; Branch, R. W.; Nicolau, D. V.; Pilizota, T.; Steel, B. C.; Maini, P. K.; Berry, R. M. *Science* **2010**, *327*, 685. (c) Freiburger, L. A.; Baettig, O. M.; Sprules, T.; Berghuis, A. M.; Auclair, K.; Mittermaier, A. K. *Nat. Struct. Mol. Biol.* **2011**, *18*, 288. (d) Mullen, M. A.; Assmann, S. M.; Bevilacqua, P. C. *J. Am. Chem. Soc.* **2012**, *134*, 812. (e) Weinkam, P.; Pons, J.; Sali, A. *Proc. Natl. Acad. Sci. U.S.A.* **2012**, *109*, 4875. (f) Zhou, L. *Nat. Chem. Biol.* **2012**, *8*, 136. (g) Reichow, S. L.; Clemens, D. M.; Freites, J. A.; Nemeth-Cahalan, K. L.; Heyden, M.; Tobias, D. J.; Hall, J. E.; Gonen, T. *Nat. Struct. Mol. Biol.* **2013**, *20*, 1085. (h) Ferreon, A. C. M.; Ferreon, J. C.; Wright, P. E.; Deniz, A. A. *Nature* **2013**, *498*, 390.

(2) (a) Ackers, G. K.; Doyle, M. L.; Myers, D.; Daugherty, M. A. *Science* **1992**, *255*, 54. (b) Lukin, J. A.; Ho, C. *Chem. Rev.* **2004**, *104*, 1219. (c) Alcantara, R. E.; Xu, C.; Spiro, T. G.; Guallar, V. *Proc. Natl. Acad. Sci. U.S.A.* **2007**, *104*, 18451. (d) Nagatomo, S.; Nagai, M.; Kitagawa, T. *J. Am. Chem. Soc.* **2011**, *133*, 10101. (e) Levantino, M.;

Spilotros, A.; Cammarata, M.; Schiro, G.; Ardiccioni, C.; Vallone, B.; Brunori, M.; Cupane, A. *Proc. Natl. Acad. Sci. U.S.A.* **2012**, *109*, 14894.
(3) Harman, J. G. *Biochim. Biophys. Acta* **2001**, *1547*, 1.
(4) (a) Perlmutter-Hayman, B. *Acc. Chem. Res.* **1986**, *19*, 90. (b) Taylor, P. N.; Anderson, H. L. *J. Am. Chem. Soc.* **1999**, *121*, 11538. (c) Thordarson, P.; Bijsterveld, E. J. A.; Elemans, J.; Kasak, P.; Nolte, R. J. M.; Rowan, A. E. *J. Am. Chem. Soc.* **2003**, *125*, 1186. (d) Thordarson, P.; Coumans, R. G. E.; Elemans, J. A. A. W.; Thomassen, P. J.; Visser, J.; Rowan, A. E.; Nolte, R. J. M. *Angew. Chem., Int. Ed.* **2004**, *43*, 4755. (e) Webb, J. E. A.; Crossley, M. J.; Turner, P.; Thordarson, P. *J. Am. Chem. Soc.* **2007**, *129*, 7155. (f) Chekmeneva, E.; Hunter, C. A.; Packer, M. J.; Turega, S. M. *J. Am. Chem. Soc.* **2008**, *130*, 17718. (g) Deutman, A. B. C.; Monnereau, C.; Moalin, M.; Coumans, R. G. E.; Veling, N.; Coenen, M.; Smits, J. M. M.; de Gelder, R.; Elemans, J. A. A. W.; Ercolani, G.; Nolte, R. J. M.; Rowan, A. E. *Proc. Natl. Acad. Sci. U.S.A.* **2009**, *106*, 10471. (h) Xu, H.; Zuend, S. J.; Woll, M. G.; Tao, Y.; Jacobsen, E. N. *Science* **2010**, *327*, 986. (i) Hogben, H. J.; Sprafke, J. K.; Hoffmann, M.; Pawlicki, M.; Anderson, H. L. *J. Am. Chem. Soc.* **2011**, *133*, 20962. (j) Hunter, C. A.; Misuraca, M. C.; Turega, S. M. *Chem. Sci.* **2012**, *3*, 589. (k) Valderrey, V.; Escudero-Adán, E. C.; Ballester, P. *Angew. Chem., Int. Ed.* **2013**, *52*, 6898.
(5) (a) Tsai, C. J.; del Sol, A.; Nussinov, R. *J. Mol. Biol.* **2008**, *378*, 1. (b) Hunter, C. A.; Anderson, H. L. *Angew. Chem., Int. Ed.* **2009**, *48*, 7488. (c) Ercolani, G.; Schiaffino, L. *Angew. Chem., Int. Ed.* **2011**, *50*, 1762. (d) Hunter, C. A.; Misuraca, M. C.; Turega, S. M. *J. Am. Chem. Soc.* **2011**, *133*, 582. (e) Fasting, C.; Schalley, C. A.; Weber, M.; Seitz, O.; Hecht, S.; Koksch, B.; Dernedde, J.; Graf, C.; Knapp, E. W.; Haag, R. *Angew. Chem., Int. Ed.* **2012**, *51*, 10472. (f) Kremer, C.; Lützen, A. *Chem.—Eur. J.* **2013**, *19*, 6162.
(6) (a) Connors, K. A.; Paulson, A.; Toledo-Velasquez, D. *J. Org. Chem.* **1988**, *53*, 2023. (b) Connors, K. A. In *Comprehensive Supramolecular Chemistry*; Atwood, J. L., Davies, J. E. D., MacNicol, D. D., Vögtle, F., Lehn, J.-M., Eds.; Pergamon: Oxford, 1996; Vol. 3, p 205. (c) Thordarson, P. *Chem. Soc. Rev.* **2011**, *40*, 1305. (d) Thordarson, P. In *Supramolecular Chemistry: From Molecules to Nanomaterials*; Gale, P., Steed, J., Eds.; John Wiley & Sons: Chichester, UK, 2012; Vol. 2, p 239.
(7) (a) Kim, S. K.; Sessler, J. L. *Chem. Soc. Rev.* **2010**, *39*, 3784. (b) McConnell, A. J.; Beer, P. D. *Angew. Chem., Int. Ed.* **2012**, *51*, 5052.
(8) (a) Lankshear, M. D.; Cowley, A. R.; Beer, P. D. *Chem. Commun.* **2006**, 612. (b) Lankshear, M. D.; Dudley, I. M.; Chan, K.-M.; Cowley, A. R.; Santos, S. M.; Felix, V.; Beer, P. D. *Chem.—Eur. J.* **2008**, *14*, 2248. (c) Perraud, O.; Robert, V.; Martinez, A.; Dutasta, J.-P. *Chem.—Eur. J.* **2011**, *17*, 4177. (d) Ciardi, M.; Tancini, F.; Gil-Ramírez, G.; Escudero Adán, E. C.; Massera, C.; Dalcanale, E.; Ballester, P. *J. Am. Chem. Soc.* **2012**, *134*, 13121. (e) Romański, J.; Piątek, P. *J. Org. Chem.* **2013**, *78*, 4341.
(9) (a) Deetz, M. J.; Shang, M.; Smith, B. D. *J. Am. Chem. Soc.* **2000**, *122*, 6201. (b) Mahoney, J. M.; Beatty, A. M.; Smith, B. D. *J. Am. Chem. Soc.* **2001**, *123*, 5847. (c) Mahoney, J. M.; Davis, J. P.; Beatty, A. M.; Smith, B. D. *J. Org. Chem.* **2003**, *68*, 9819. (d) Tumcharern, G.; Tuntulani, T.; Coles, S. J.; Hursthouse, M. B.; Kilburn, J. D. *Org. Lett.* **2003**, *5*, 4971. (e) Smith, B. D. In *Macrocyclic Chemistry: Current Trends and Future Perspectives*; Gloe, K., Ed.; Springer: Dordrecht, The Netherlands, 2005; p 137. (f) Chae, M. K.; Lee, J.-I.; Kim, N.-K.; Jeong, K.-S. *Tetrahedron Lett.* **2007**, *48*, 6624. (g) Lankshear, M. D.; Dudley, I. M.; Chan, K.-M.; Beer, P. D. *New J. Chem.* **2007**, *31*, 684. (h) Sessler, J. L.; Kim, S. K.; Gross, D. E.; Lee, C.-H.; Kim, J. S.; Lynch, V. M. *J. Am. Chem. Soc.* **2008**, *130*, 13162. (i) Kim, S. K.; Sessler, J. L.; Gross, D. E.; Lee, C.-H.; Kim, J. S.; Lynch, V. M.; Delmau, L. H.; Hay, B. P. *J. Am. Chem. Soc.* **2010**, *132*, 5827. (j) Park, I.-W.; Kim, S.-K.; Lee, M.-J.; Lynch, V. M.; Sessler, J. L.; Lee, C.-H. *Chem.—Asian J.* **2011**, *6*, 2911. (k) Kim, S. K.; Vargas-Zúñiga, G. I.; Hay, B. P.; Young, N. J.; Delmau, L. H.; Masselin, C.; Lee, C.-H.; Kim, J. S.; Lynch, V. M.; Moyer, B. A.; Sessler, J. L. *J. Am. Chem. Soc.* **2012**, *134*, 1782. (l) Park, I.-W.; Yoo, J.; Kim, B.; Adhikari, S.; Kim, S. K.; Yeon, Y.; Haynes, C. J. E.; Sutton, J. L.; Tong, C. C.; Lynch, V. M.; Sessler, J. L.; Gale, P. A.; Lee, C.-H. *Chem.—Eur. J.* **2012**, *18*, 2514. (m) Kim, S. K.; Hay, B. P.; Kim, J. S.; Moyer, B. A.; Sessler, J. L. *Chem. Commun.* **2013**, *49*, 2112.
(10) (a) Redman, J. E.; Beer, P. D.; Dent, S. W.; Drew, M. G. B. *Chem. Commun.* **1998**, 231. (b) Eckelmann, J.; Saggiomo, V.; Sonnichsen, F. D.; Luning, U. *New J. Chem.* **2010**, *34*, 1247. (c) Moerkerke, S.; Ménand, M.; Jabin, I. *Chem.—Eur. J.* **2010**, *16*, 11712. (d) Sleem, H. F.; Dawe, L. N.; Georghiou, P. E. *New J. Chem.* **2012**, *36*, 2451. (e) Moerkerke, S.; Le Gac, S.; Topić, F.; Rissanen, K.; Jabin, I. *Eur. J. Org. Chem.* **2013**, *2013*, 5315.
(11) Lowe, A. J.; Pfeffer, F. M.; Thordarson, P. *Supramol. Chem.* **2012**, *24*, 585.
(12) Gryko, D. T.; Pęcak, A.; Koźmiński, W.; Piątek, P.; Jurczak, J. *Supramol. Chem.* **2000**, *12*, 229.
(13) (a) Kavallieratos, K.; deGala, S. R.; Austin, D. J.; Crabtree, R. H. *J. Am. Chem. Soc.* **1997**, *119*, 2325. (b) Kavallieratos, K.; Bertao, C. M.; Crabtree, R. H. *J. Org. Chem.* **1999**, *64*, 1675.
(14) Gale, P. A. *Acc. Chem. Res.* **2006**, *39*, 465.
(15) (a) Hofmeister, F. *Arch. Exp. Pathol. Pharmakol.* **1888**, *24*, 247. (b) Lo Nostro, P.; Ninham, B. W. *Chem. Rev.* **2012**, *112*, 2286.
(16) Gutmann, V. *The Donor-Acceptor Approach to Molecular Interactions*; Plenum Press: New York, 1978.
(17) Izatt, R. M.; Bradshaw, J. S.; Nielsen, S. A.; Lamb, J. D.; Christensen, J. J.; Sen, D. *Chem. Rev.* **1985**, *85*, 271.
(18) Junk, P. C.; Steed, J. W. *J. Coord. Chem.* **2007**, *60*, 1017.
(19) Wilcox, C. S. In *Frontiers in Supramolecular Organic Chemistry and Photochemistry*; Schneider, H.-J., Dürr, H., Eds.; VCH: Weinheim, 1991; p 123.
(20) Connors, K. A. *Chem. Rev.* **1997**, *97*, 1325.
(21) (a) Monod, J.; Changeux, J. P.; Jacob, F. *J. Mol. Biol.* **1963**, *6*, 306. (b) Monod, J.; Wyman, J.; Changeux, J. P. *J. Mol. Biol.* **1965**, *12*, 88. (c) Cui, Q.; Karplus, M. *Protein Sci.* **2008**, *17*, 1295.